

Research Article

GIS-based route planning in landslide-prone areas

A. K. SAHA[†], M. K. ARORA[‡], R. P. GUPTA^{*†}, M. L. VIRDI[‡] and
E. CSAPLOVIC[§]

[†]Department of Earth Sciences, Indian Institute of Technology Roorkee,
Roorkee 247667, India

[‡]Department of Civil Engineering, Indian Institute of Technology Roorkee,
Roorkee 247667, India

[§]Institute of Photogrammetry and Remote Sensing, Department of Geosciences,
Dresden University of Technology, Dresden 01062, Germany

(Received 10 September 2004; in final form 20 December 2004)

Many parts of the world with young mountain chains, such as the Himalayas, are highly susceptible to landslides. Due to general ruggedness and steep slopes, roads provide the only way of transportation and connectivity in such terrains. Generally, landslide hazards are overlooked during route planning. In this study, in a test area in the Himalayas, various thematic layers, viz. landslide distribution, landslide hazard zonation, landuse/landcover, drainage order and lithology are generated and integrated using Remote Sensing–GIS techniques. The integrated data layer in raster form has been called a ‘thematic cost map’ and provides an estimate of the cost of route development and maintenance. The relative cost assignment is based on experts’ knowledge. Route planning is based on neighbourhood analysis to find various movement possibilities from a pixel to its immediate neighbours. A number of patterns such as those analogous to movements in chess games have been considered. Two new neighbourhood patterns, named here Knight31 and Knight32, have been conceived in addition to commonly used Rook, Bishop and Knight patterns. The neighbourhood movement cost for moving from one pixel to a connected neighbour has been calculated for a 7×7 pixel window considering distance, gradient cost and thematic cost. Dijkstra’s algorithm has been applied to compute the least-cost route between source and destination points. A few examples are presented to show the utility of this approach for a landslide-safe automatic route planning for a highly rugged hilly terrain.

Keywords: Route planning; Landslide; Remote Sensing; GIS

1. Introduction

The Himalayan terrain is highly susceptible to landslides, mainly owing to its complex geological setting combined with contemporary crustal movements, high relief and heavy rainfall. Due to general ruggedness of the terrain and steep slopes, roads provide the only way of transportation and connectivity in the Himalayan region. Invariably, in the rainy seasons, some sections of the roads are blocked due to landslides, thereby disconnecting many villages and towns. Every year, a huge

*Corresponding author. Email: rpgesfes@iitr.ernet.in

amount of money is spent in road maintenance. Hence, there is a great need for effective route planning, which is efficient in engineering design and also considers various geological factors in terms of slope stability and safety.

The conventional route planning has solely been based on topographical considerations—gradient and curvature. Usual practice involves manually marking segments of permissible gradients for route alignment on large-scale topographical maps. Such an approach is cumbersome and tedious, and thus may not be feasible when a variety of other factors such as landslides, geology and landuse/landcover are also considered.

With the availability of data from remote sensing satellites, it has become possible to efficaciously collect and analyse synoptic spatial data, such as geology, structural features, landuse/landcover, drainage, settlements, etc. Besides, advanced Geographic Information System (GIS) computational techniques offer numerous advantages in multi-geodata handling for integrated geoenvironmental studies. The main aim of this paper is to present the potential of remote sensing–GIS technology to devise an automatic and intelligent approach for route planning in hilly regions that are prone to landslides.

2. Route planning using GIS—a review

During the last decade, a few attempts have been made to automate the route-planning process using GIS technology. A review of a number of papers suggests that the methodology is still at an exploratory stage. Moreover, due to the complexity of the problem, the proposed methods have not been tested in very high altitude rugged terrains, such as the Himalayas.

Both vector and raster GIS may be applied. In a raster GIS, the flexibility in the selection of neighbourhood pattern is rather limited as compared to a vector GIS. However, the thematic cost computation is easy to conceive and manipulate in raster GIS. Moreover, remote sensing data, which form a link to many datasets, are also in raster format; raster GIS becomes an automatic choice.

Dijkstra's algorithm has been widely used for finding the least-cost path. This algorithm is designed for tracing the shortest path in a network with nodes connected by weighted links. In a raster GIS, the centre of each pixel is considered as a node. A few modifications of this algorithm have been reported for specific applications. A* (pronounced 'Eh star') algorithm (Tanimeto 1987) is a variation of Dijkstra's algorithm (Dijkstra 1959), which uses some heuristic information related to the node or pixel of interest. As Dijkstra's algorithm is computationally intensive and requires a huge memory for data storage to find the shortest path, the computational process slows down. To improve the computational efficiency, a parallel Dijkstra algorithm with constraints has been developed by Solka *et al.* (1995), which uses the concept of neural network for optimization.

In the late 1980s and early 1990s, the 'G-ROUTE' package in raster GIS environment developed by ITC (Ellis 1990) has been used for least-cost route planning by some workers. The package considers various road-construction parameters, namely distance and gradient, roadfill, drainage crossing and arable land possession costs. These parameters are integrated, and finally Dijkstra's Algorithm is implemented to find the least-cost path. The package uses the simplest form of neighbouring pattern in a 3×3 pixel window. Examples of 'G-ROUTE' application can be found in Akinyede (1990) for highway route planning and in Schneider and Robbins (1998) for modelling access to health care centres in the

Nepal Himalayas. There are a few other commercial software packages which contain appropriate route-planning modules that generate the least-cost path. These include PATHDISTANCE in ArcGIS, VARCOST and PATHWAY in IDRISI. However, the neighbourhood search is limited to a 3×3 pixel matrix only in these modules.

In a 3×3 pixel matrix, a maximum of eight neighbourhood directions, and in a 5×5 pixel matrix, 16 neighbourhood directions are possible. The use of these neighbourhoods for cost computation may, however, result in rather sharp zigzag and unrealistic paths. To overcome this problem, to a certain extent, Xu and Lathrop (1994) used an anisotropic (elliptical) spread function in GRASS (a raster GIS) for neighbourhood path selection to incorporate any number of non-adjacent pixels to make the path smoother and showed implementation of the procedure to wildfire spread. The limitation of this method for route planning in a rugged hilly terrain would be due to sudden variation of gradient over short distances.

In a real-world problem on pipeline routing in the Caspian sea region, Feldman *et al.* (1995) utilized remote sensing and GIS tools to model costs associated with terrain conditions, geology, landuse, etc. The costs were computed based on the experience of various earlier pipeline projects. The Spatial Analyst module of ARC/INFO GIS software was used to extract the least-cost pipeline route from a cumulative cost surface. It was shown that the least-cost path derived in this study was 21% longer than the straight-line path between the source and destination, but it led to a reduction in pipeline construction costs of 14%.

Lee and Stucky (1998) applied viewshed analysis for determining least-cost paths, which can be utilized for civil engineering, military and environmental planning activities. They formulated four different types of viewpaths from a digital elevation model, which were named as hidden path, scenic path, strategic path and withdrawn path. The visibility cost for various viewpaths, surface distance and gradient, were used together for calculating the cost of movement from the source to its nearest eight neighbouring pixels. Finally, the least-cost path between source and destination was determined using an iterative searching procedure formulated by Douglas (1994). Lee and Stucky (*op. cit.*) tested this algorithm for hiking and pipeline layout problems using a $30\text{ m} \times 30\text{ m}$ USGS Digital Elevation Model (DEM). However, in their study, the maximum allowed gradient for path selection was considered as 50° , which was too high for a realistic road alignment. Moreover, only slope, distance and viewshed factors were considered, and no other thematic parameters, e.g. cost of land, geology, landslide, etc., were taken into account.

Collischonn and Pilar (2000) presented an algorithm based on dynamic programming to find direction-dependent least-cost path for roads and canals. The algorithm considers costs associated with eight neighbours of a source pixel (i.e. 3×3 pixel window) based on gradient and distance. The main emphasis was given to gradient constraints for the purpose of canal alignment, and the algorithm was tested on a few hypothetical terrains.

In another study, Musa and Mohamed (2002) presented a best-path model for forest road network, in which road alignments were generated using three different methods: manual, field survey and computer-GIS. A comparative study showed that the path generated by the computer-GIS method was better than the other two and was of immense help to the planners.

Yu *et al.* (2003) presented a comprehensive review of the problem on route alignment in GIS and also extended the work based on a least-cost algorithm for

roadway planning. Various possibilities of network neighbours using a 5×5 pixel window were presented, which were named after the moves in a game of chess, viz. the Rook's, Queen's and Knight's patterns. A cost function was derived to cumulate gradient cost and landuse/landcover cost with distance. Finally, Dijkstra's algorithm was used to find the least-cost path between the source and the destination points. Further, a new technique, called the Smart Terrain (ST) algorithm, was also adopted to propose the location of bridges and tunnels using contour information. The methodology was tested using a $30\text{ m} \times 30\text{ m}$ USGS DEM and landcover information derived from satellite images. The results showed that the ST algorithm produced a more realistic least-cost route by using spatial distance, anisotropic cumulated cost and location of bridges and tunnels. They also showed an improvement in the character of the path after incorporating the Knight's pattern, as the earlier approaches used only the Queen's pattern.

In a more recent study on finding least-cost footpaths in a mountainous terrain, Rees (2004) used an optimized metabolic cost for human locomotion based on Naismith's Rule (Fritz and Carver 1998) along with a distance function. Dijkstra's Algorithm was used to find the least-cost path between the selected locations, which was compared with the existing footpaths in the region.

This review clearly states the usefulness of remote sensing-GIS tools coupled with computer-based algorithms for various kinds of route planning studies. In this paper, the work of Yu *et al.* (2003) has further been expanded to generate least-cost paths for route planning in Himalayan region susceptible to landslides.

3. Methodology overview

The general methodology of the proposed route-planning approach adopted is shown in figure 1. It involves a collection of data from a number of sources including

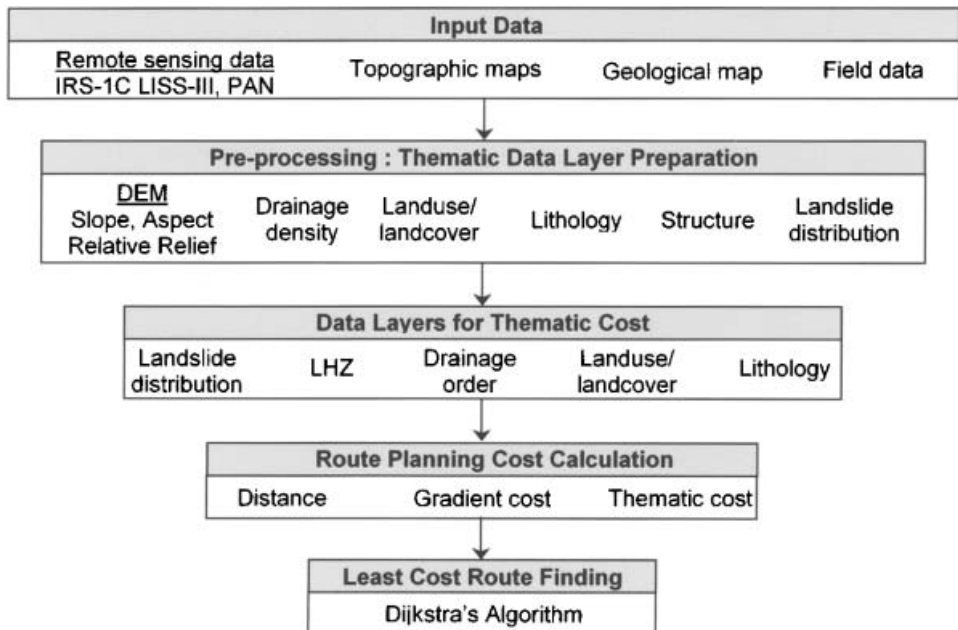


Figure 1. Overview of the methodology adopted.

topographic maps, geological maps, remote sensing data, etc. Pre-processing of remote sensing data was carried out for removal of common radiometric and geometric distortions. A number of thematic data layers for various factors related to landslide activity were generated, and a landslide hazard zonation (LHZ) map was prepared. A concept of thematic cost map for route development and maintenance was developed, and various thematic data layers were integrated in a GIS environment to generate a 'thematic cost' map. This was followed by computation of 'neighbourhood movement cost' (i.e. cost of moving from a source pixel to its possible connected neighbours), considering direction-dependent terrain gradient, distance and the thematic cost. Subsequently, Dijkstra's Algorithm was adopted and implemented for least-cost route selection. Finally, testing of the developed approach in different terrain conditions in the study area has been carried out.

Remote sensing data from IRS-1C LISS-III and PAN sensors have been primarily used for generating various thematic data layers. Survey of India toposheets have been used to prepare a base map. Published and field data on geology, structure, landslides, landuse/landcover and GCPs have been collected and integrated with remote sensing data. Various software packages (ERDAS Imagine 8.6 and ILWIS 3.2) have been used for data processing. A dedicated software (LaSIRF) in C++ language has been developed for least-cost path identification and has been suitably interfaced with the ILWIS GIS software.

4. Study area

In order to develop and test the approach, a landslide-prone study area covering about 550 km² in the Chamoli and Rudraprayag districts of Uttaranchal State in the Himalayas, India has been selected (figure 2). The terrain is highly rugged with elevations ranging from 920 to 4250 m above mean sea level (msl). The Alaknanda river and its tributaries constitute the drainage network of the area and represent a young stage of geomorphological development with steep slopes and high runoff. There is a marked spatial variation in the type and density of vegetation. In general, the south-facing slopes are more vegetated than the north-facing slopes owing to differential solar insolation. The high-altitude areas are snow-covered, and paddy cultivation is usually practised on the terraces of hill slopes.

Geologically, the area falls mainly in the Lesser Himalayas with a part lying in the Higher Himalayas. The Main Central Thrust (MCT) passing through the northern part of the study area separates the rocks of the Lesser Himalayas from those of Higher Himalayas. In this work, the regional geology is adopted from Valdiya (1980). The rocks exposed are various types of mainly metamorphic rocks such as gneisses, schists, granites, quartzites, slates, some limestones and dolomites. Structurally, the study area is highly complex with several thrusts and folds. There are two major thrusts that pass through this area along which the rocks are highly crushed and sheared. Several irregularly oriented faults are also present in the area.

5. Data used

The study has utilized three main types of data: (1) remote sensing data, (2) ancillary data and (3) field data. The remote sensing data from the Indian Remote Sensing satellite (IRS-1C), sensors LISS-III and PAN have been used.

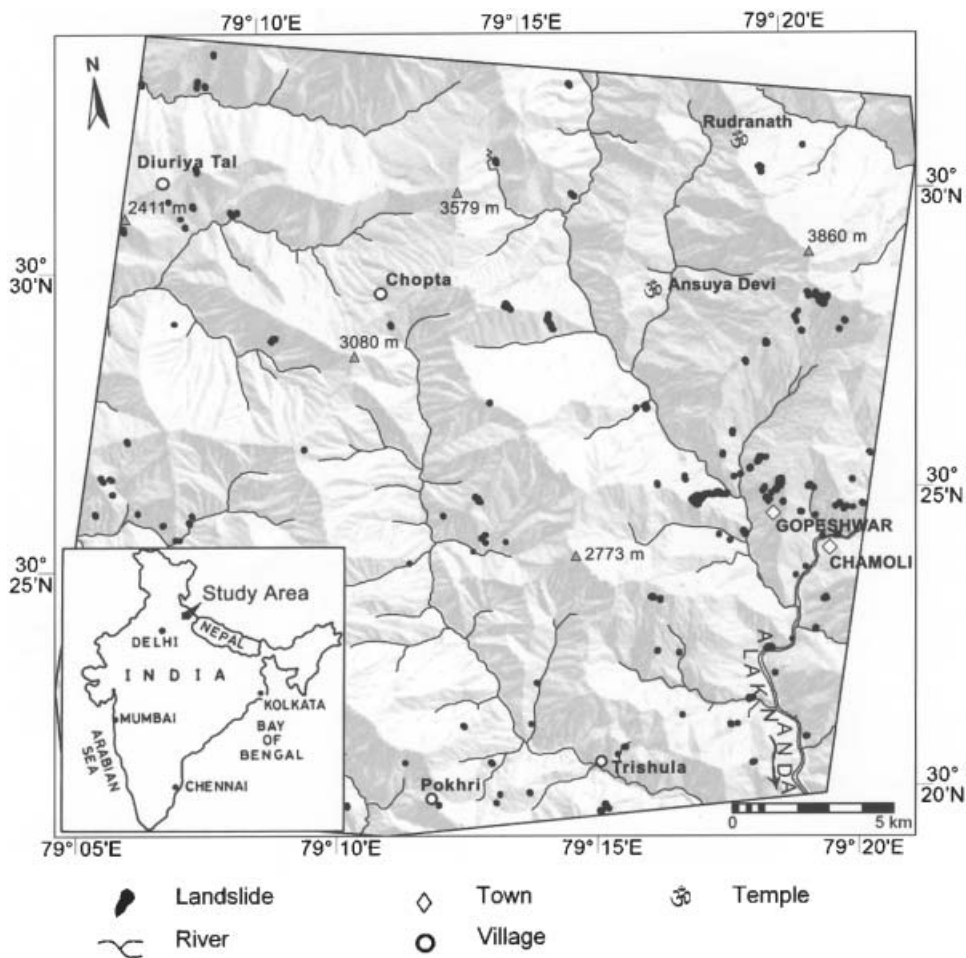


Figure 2. Location map of the study area (the background is a shaded relief model).

LISS-III sensor provides multispectral data at 23.5 m spectral resolution in four bands, viz. green, red, near-infrared (NIR) and shortwave infrared (SWIR). The panchromatic camera provides data in a single broad band with a spatial resolution of 5.8 m. These remote sensing data have been used for mapping of landuse/landcover, lineament and existing landslides. The remote sensing images have been geometrically corrected and accurately registered with topographic map using a large number of well-distributed GCPs and the method of 'rubber sheet-stretching' (Gupta 2003). The multispectral remote sensing data have been corrected for atmospheric path radiance using the 'dark-object subtraction' technique (e.g. Chavez 1988, Gupta 2003).

The ancillary data, namely topographical and geological maps, and road design parameters have been collected from various sources. A large amount of information has been extracted from the topographic maps, e.g. contours and point elevations, drainage network, roads, etc. A geological map (after Valdiya 1980) has been used to collect information on lithology and structural features, e.g. thrusts and faults. The hill road design parameters (after Indian Roads Congress, IRC: 52-2001) have been used in planning the route.

Field data are very important in any remote sensing–GIS study. Sufficient field data have also been collected to obtain information on lithology, structure, geology, existing landslide distribution and to collect training and testing data samples for landuse/landcover classification and distribution.

6. Pre-processing and thematic data layer preparation

Generation of thematic data layers has been an important task in this study. A number of thematic data layers, viz. DEM, lithology, landuse/landcover, drainage order, landslide distribution and landslide hazard zonation (LHZ), have been generated using remote sensing–GIS techniques.

6.1 Digital elevation model

A digital elevation model (DEM) is a basic component in GIS analysis. In this study, the conventional topographic map digitization technique has been implemented to generate the DEM. Contours from the Survey of India topographic map have been digitized, rasterized, and interpolated to generate the DEM. Various DEM-based derivatives, such as slope, aspect, and relative relief have then been produced.

6.2 Lithology

The regional geological map has been used as the basic input. The rock groups and formations are reclassified into five major lithounits, viz. quartzites intercalated slates, schists and gneisses, limestones and greywackes, granite-granodiorite-gneisses, and granites. The geological map has been digitized and co-registered with other thematic layers.

6.3 Structural features

Structural features include thrusts, faults and lineaments, which are very important in landslide studies. These structural features describe the zone/plane of weakness, shearing and tectonic activity along which landslide susceptibility is higher. The map showing structural features has been prepared by integrating the existing geological map with the structural lineaments interpreted from remote sensing data. As the incidence of landslide decreases with increasing distance from structural features, a buffer zone has been created along each structural feature and sliced with respect to distance (504 m each).

6.4 Drainage

A drainage map has been generated by digitizing the drainage lines from the topographical maps and has subsequently been used for generating drainage density maps and drainage order maps. The drainage density map has been used as an input for the generation of LHZ map, whereas the drainage order map has been used later to estimate the cost of bridge construction, if required, during route planning.

6.5 Landuse/landcover

Remote sensing data are particularly useful in mapping landuse/landcover in mountainous regions, such as the Himalayas. In such a terrain, classification of

remote sensing data encounters many problems due to the presence of shadows, low sun angle, steep slopes and differential vegetation cover. Therefore, a multi-source classification approach (Arora and Mathur 2001) has been adopted. The multi-spectral LISS-III image from IRS-1C together with Normalized Difference Vegetation Index (NDVI) and DEM have been used as the input data sources for Maximum Likelihood Classification (MLC). The IRS-1C PAN image together with information from field surveys served as reference data for generating training and testing areas. A number of classes have been mapped, viz. dense forest, sparse vegetation, agricultural land, fallow land, barren land, settlements, fresh sediments, water body and snow. A landuse/landcover map with an accuracy of 92.06% has been achieved and used as the data layer (for details, see Saha *et al.* 2005a).

6.6 *Landslide mapping*

In this study, particular emphasis has been given to existing landslides and landslide hazard zonation and their impact on route planning; hence, accurate mapping of landslides is very important.

6.6.1 Mapping of existing landslides. In high-altitude mountainous regions, landslides occur at distant and remote places, therefore remote sensing is a very valuable tool in landslide mapping. A high-resolution PAN image and PAN-sharpened multi-spectral image have been used to identify and map the existing landslides. The identification and recognition of landslides have been carried out based on tone/colour, shape, landform, drainage and vegetation. A total of 190 landslides of varying dimensions have been mapped from remote sensing data. Many of these landslides have been field-checked.

6.6.2 Landslide hazard zonation. Landslide hazard zonation (LHZ) deals with segmenting an area into near-homogeneous domains and ranking these according to degrees of potential landslide hazard (Varnes 1984). For many years, remote sensing–GIS techniques have been used for LHZ mapping (e.g. Gupta and Joshi 1990, Nagarajan *et al.* 1998, Saha *et al.* 2002, Arora *et al.* 2004). In this study, a number of thematic maps, related to landslide activity (as described above), viz. structural features, lithology, relative relief, slope, aspect, landcover and drainage density have been generated and used as inputs for LHZ mapping. To evaluate the contribution of each of the above factors in landslide hazard, weights have been computed using the existing landslide distribution data layer. The weighted thematic maps thus produced have been laid one over another and added to generate a Landslide Hazard Index (LHI) map in GIS. Segmentation of LHI values has been carried out by a new probabilistic approach. The LHI range has been segmented into five classes with boundaries placed on the basis of mean and standard error. A number of trials have been done, and the best LHZ map is selected on the basis of the ‘success rate curve’ method (for details, see Saha *et al.* 2005b).

7. **Data processing and analysis for route planning**

The proposed route planning procedure can be broadly divided into the following four basic steps:

1. Generating a thematic cost map: In a landslide-prone terrain such as the Himalayas, several geo-environmental factors (viz. existing landslides, potential of a new landslide occurrence, cost of land acquisition, requirement

of a possible bridge and costs of blasting, excavation and cut-and-fill works, etc.) have a direct bearing on the cost of road development and maintenance. The spatial variation of these factors can be represented in terms of raster data layers, which can be integrated in GIS to arrive at a cumulative data layer, here called the 'thematic cost map'. The thematic cost map is a raster map where value at each pixel gives the estimated relative cost of passing through the pixel.

2. Selection of connected neighbours: Based on the neighbourhood relationship concept in GIS, in a raster or grid-based model, each pixel can be represented as a network node. This step involves finding various possibilities of the connected nodes.
3. Calculation of neighbourhood movement cost (NM-cost): Once connected neighbours are found, the next step is to calculate the cost of moving to the connected neighbour from a source. This is termed here the NM-cost and is computed from three input data: cost related to neighbour-distance, cost related to gradient and the thematic cost.
4. Selection of least-cost route: As the route alignment will cover a certain distance, it will pass through pixels, and their successive NM-cost values will accumulate to give the total cost. This final step involves finding the least-cost route for which a dedicated computer program has been written in C++.

In the following sections, details of all the four steps are given. The procedure helps select an optimal route that is supposed to be the best, as it tries to avoid major landslides and passes through low thematic cost zones, thereby reducing overall road development and maintenance costs. Finally, a few examples have been presented with various terrain and landslide hazard conditions. Figure 3 shows the route planning steps adopted in this study.

7.1 Thematic cost—concept and computation

The cost of route development and maintenance is dependent upon a number of factors, the most important of these being landslide distribution, landslide hazard zonation, landuse/landcover, lithology and drainage order. The thematic cost map is defined as a raster map, where the value at each pixel gives the estimated relative cost of route development and maintenance through the pixel. The cost is cumulative, having inputs from various data layers.

The data layers, landslide distribution (size), landslide hazard zonation, drainage order, landuse/landcover and lithology are of diverse types consisting of measurements at different scales, such as categorical, ordinal and ratio type data (for details see, Aronoff 1989, for example). In order to integrate this variety of data, an ordinal weighting rating is used, and to arrive at a cumulative data layer, the concept of thematic cost is developed here (figure 4). A higher cost value at a pixel may be related to a higher cost for bridge construction, road maintenance due to landslides, land acquisition, blasting, etc. Therefore, a weighting-rating system in the range of 0 to 9 is used here, with zero signifying the minimum cost and 9 implying the highest cost.

An ordinal number, from 0 to 9, is given to each thematic data layer in terms of its relative importance. For example, the landslide distribution thematic data layer is assigned the highest weight of 9, followed by LHZ (weight=8), drainage order (weight=7), landuse/landcover (weight=6) and lithology (weight=4). Similarly,

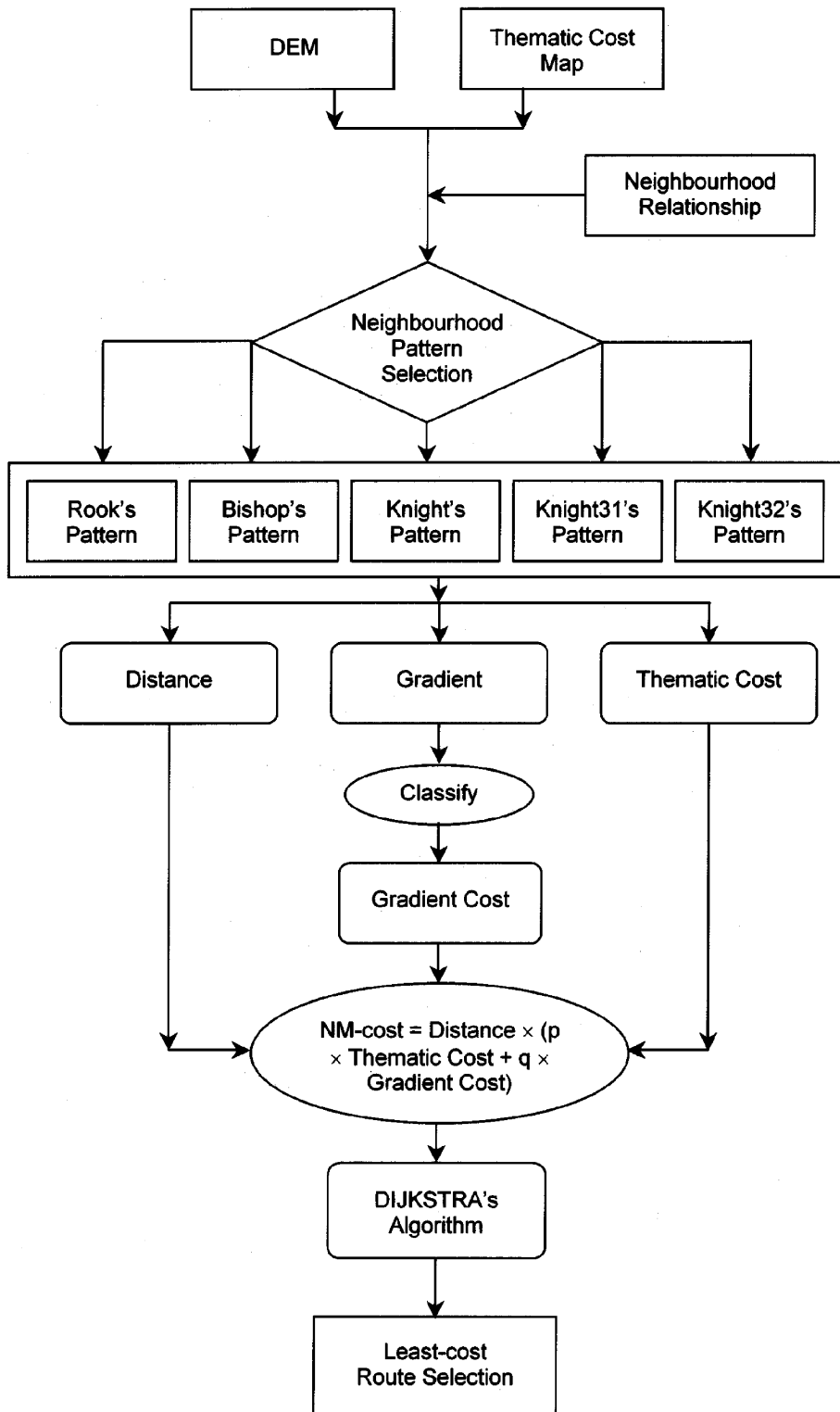


Figure 3. Route-planning methodology.

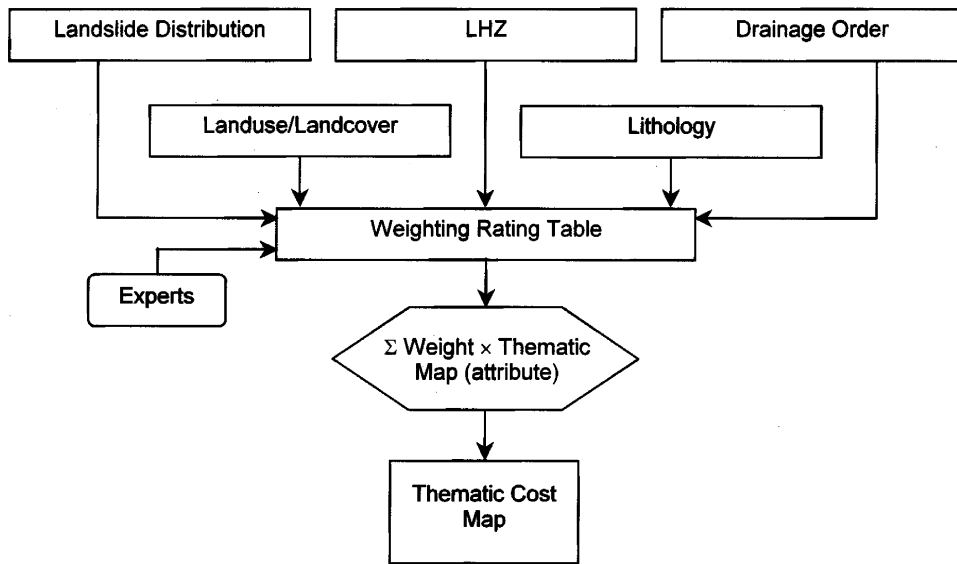


Figure 4. Schematic diagram for generating the thematic cost map used in route planning.

each class in the thematic data layer has been given an ordinal rating in the range of 0–9 (table 1). The weighting-rating values are based on a comparative study of various thematic data layers and discussions with experts working in the area of transportation engineering. The following describes the logic in brief for weighting-rating values adopted here.

7.1.1 Landslide distribution. It is considered here that landslide occurrence is the most important parameter in road planning in a mountainous terrain, as landslides lead to recurring problems, such as blockades, disruptions, civic miseries, etc., and greatly increase the cost of transport maintenance. Therefore, the highest weight of 9 has been given to landslide occurrence. There is no doubt that it may be ideal to avoid landslide areas altogether during road planning. However, if the landslides are small in size, it may be possible to apply slope-stabilization measures for the route to pass through these. Keeping this aspect in view, rating values have been assigned according to the size of the landslides in the region. The landslide map has been re-classified into six classes depending upon the size of landslides. Landslides covering more than 400 pixels (1 pixel = 36 m²) have been assigned a near-infinite value so that no road can pass through this area. Further, a buffer of 50 m around the landslide area has been provided to keep a safe distance from the landslides. If there is no landslide, the pixels have been assigned a zero value for the pixels to become favourable for road alignment. The other four landslide classes have been rated (successively 9, 8, 7 and 5) in decreasing order of size.

7.1.2 Landslide hazard zonation. The LHZ map is considered here as the second-most important parameter (weight=8) influencing the thematic cost of road development and maintenance. Each pixel in the landslide hazard zonation map prepared earlier carries a value that represents the potential of the landslide hazard. Landslide-hazard zones have been rated in increasing order according to the severity of the hazard (table 1).

Table 1. Weighting-rating scheme of thematic data layer integration.

Thematic map	Weight	Rating
<i>1. Landslide (pixels)</i>	9	
>400		∞
>300		9
>200		8
>100		7
<100		5
No Landslide		0
<i>2. Landslide Hazard Zones</i>	8	
Very High		9
High		7
Medium		5
Low		3
Very Low		1
<i>3. Drainage Order</i>	7	
6th Order		9
5th Order		8
4th Order		7
3rd Order		5
2nd Order		2
1st Order		1
No River		0
<i>4. Landuse/Landcover</i>	6	
Snow		9
Landslide Debris		9
River Sediments		7
Settlements (through)		6
Agriculture		4
Fallow Land		4
Barren Land		3
Dense Forest		3
Sparse Vegetation		1
Water Body (Deep)		1
<i>5. Lithology</i>	4	
Granite		6
Granite-Granodiorite-Gneiss		6
Schist and Gneiss		5
Quartzite with Slates		4
Limestone and Greywacke		3

7.1.3 Landuse/landcover. Landuse/landcover data are required to estimate the cost of land acquisition during route planning. In the Himalayas, the snow-covered areas occur at very high elevations, and it is difficult to construct and maintain roads at these heights. Further, the road construction over landslide debris may accentuate the problem of slope instability. Hence, snow and landslide debris-covered areas have been assigned the highest rating (=9). The areas covered with river sediments are also not suitable for road construction, as these are susceptible to flood inundation (rating=7). Sometimes, a route must pass through a settlement, which means that a higher compensation cost (rating=6) has to be provided in such cases. The agriculture and fallow lands are relatively favourable for road construction in the hills, as this kind of landuse occurs on terraces, which are regions of low relief (rating=4). Barren areas (rating=3) are relatively favourable for route planning due to the fact that such areas are under government control, involve no compensation

cost and are devoid of environmental problems like cutting of trees. Forest areas are also government lands, and a road through a forest is also likely to promote tourism; therefore, a rating of 3 has been assigned to forest areas. Sparsely vegetated areas seem to be the most suitable for road construction (rating=1). These are government land, are relatively stable, and may have minimal environmental problems.

7.1.4 Lithology. Lithology has been considered mainly from the point of view of costs of blasting, excavation, cut-and-fill works, etc. Granites and gneisses are compact and hard, and hence a higher rating (=6) has been given to granitic rocks. Successively lower cost ratings are given to schists and gneisses (=5), quartzites with slates (=4), and limestone and greywacke (=3).

7.1.5 Drainage order. The drainage-order map has been used here to consider the cost of a possible bridge construction. Generally, the width of the river channel increases with increasing order of drainage, which results in a corresponding increase in the cost of bridge construction. The drainage order map based on Strahler's (1964) scheme has been used here as an input. The first- and second-order drainages have been assigned very low ratings, as these are generally quite narrow, and in most cases the water may be drained using underground pipes, or by providing small culverts. For higher-order drainages, there may be requirements for bridge construction; the construction cost increases with the width of the channel. Therefore, higher ratings have been assigned to higher-order streams. The pixels without any channel have been assigned a zero value.

7.1.6 Thematic cost map generation. For each thematic data layer, there is a weight factor. The classes within each thematic data layer carry a rating, which is used as 'attribute data'. A large number of methodologies are available to find the interrelation among the weights and to accumulate various data layers, viz. Weighted Linear Combination, Multi Criteria Evaluation, etc. (Voogd 1983). For simplicity, the thematic cost map is computed here as:

$$\text{Thematic Cost} = \sum \text{Weight} \times \text{Thematic Data Layer (attribute)} \quad (1)$$

Hence, in this case,

$$\text{Thematic Cost} = [9 \times \text{LD} + 8 \times \text{LHZ} + 7 \times \text{DO} + 6 \times \text{LULC} + 4 \times \text{LI}] \quad (2)$$

where LD is the landslide distribution map, LHZ is the landslide hazard zonation map, DO is the drainage order map, LULC is the landuse/landcover map, and LI is the lithology map. Figure 5 represents the thematic cost map of the study area. In this map, the thematic cost values have been found to vary between 30 and 220. Lower values indicate favourable pixel sites for route planning, whereas higher values indicate relatively unfavourable or less favourable sites.

For route alignment, particularly in a hilly region, topography plays a very important role. The next section deals with the methodology incorporating the thematic cost factor, distance factor and gradient factor for route planning along with least-cost route selection.

7.2 Selection of connected neighbours

In GIS, the term 'neighbourhood' is defined as the location within proximity of some starting-point or grid cell. Neighbourhood analysis is important in route

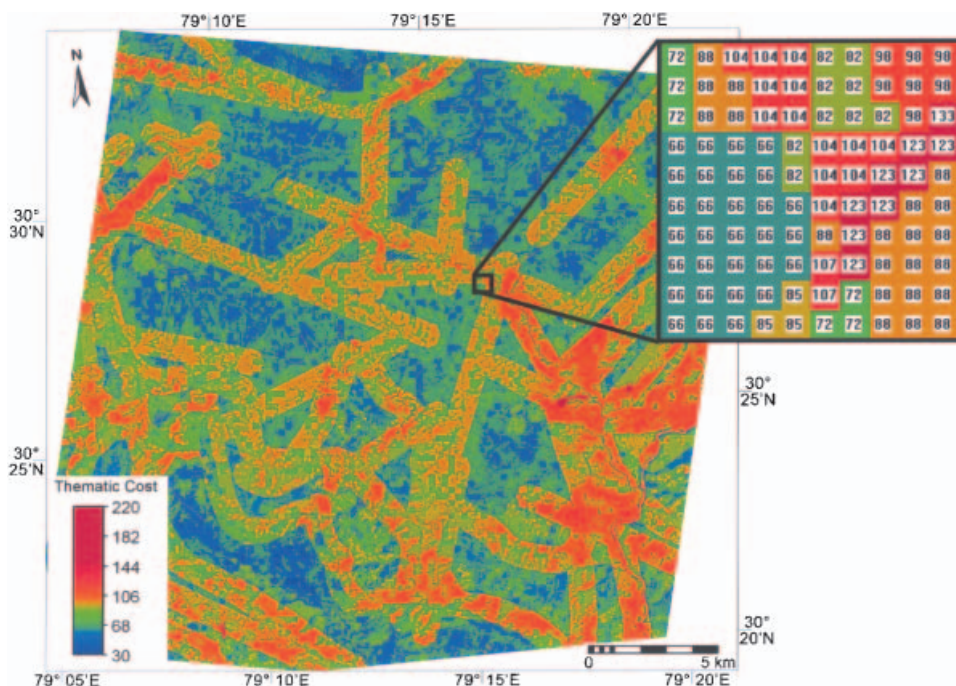


Figure 5. Thematic cost map. Each pixel value indicates the relative cost to move through the pixel; the higher the value, the higher the cost for route development and maintenance.

planning to find various possibilities of movement from a source pixel to its immediate neighbour, so that the cost associated with that connection can be calculated. The neighbourhoods may be of two types: direct neighbour and indirect neighbour.

Direct neighbours are those which are connected directly (bodily) to the source pixel. In a 3×3 pixel window, there are eight direct neighbours (two horizontal, two vertical and four diagonal) (figure 6). An analogy can be established between these connections and the moves in a game of chess. The vertical and horizontal movements are similar to the moves of the Rook, and the diagonal movements are similar to those of the Bishop. In other words, all the direct neighbours are represented as the Queen's pattern of movement (Xu and Lathrop 1994, Yu *et al.* 2003). Hence, in such cases, the turn angle interval (angle between an incoming and outgoing paths at a pixel) for the route is restricted to a minimum 45° angle.

The turn-angle interval may be reduced by considering a larger neighbourhood window. With a 5×5 pixel window, eight more indirect neighbourhood connections may be incorporated (figure 6). The indirect connection means that the pixels are not bodily connected, but a movement through this connection is allowed. These connections can be compared with the move of the Knight in a game of chess. The Knight moves two squares straight and one square left or right in the direction of movement, to occupy the new position. Hence, in such cases, the turn angle interval will be further improved to a minimum of 22.5° . This will make the path smoother. As the neighbourhood pixel window increases, the minimum turn-angle interval is improved further, but this will add to the computational cost.

In this study, up to 7×7 pixel window sizes have been considered, and two new patterns of indirect neighbourhood connections have been conceived. Although, these moves do not exist in the game of chess, these originate from the concept of the Knight's movement and therefore have been named as Knight31 and Knight32 (figure 6).

1. Knight31's pattern: The Knight31's pattern works in a 7×7 pixel window. The movements are such that it moves three pixels straight and then one pixel to the left or right.
2. Knight32's pattern: The Knight32's pattern is another new pattern designed for 7×7 pixel window. It moves three pixels straight and then two pixels to the left or right.

The two new patterns would permit smoother turns and gentler gradients in route alignment. To implement the connectivity of possible neighbours in a raster GIS platform, the pixels are represented as nodes having unique identification numbers. A mathematical relationship is used to determine the neighbourhood with adjacent pixels (or nodes). This process has been adequately programmed in C++.

7.3 Neighbourhood movement cost (NM-cost)

As mentioned earlier, usually the distance and the gradient are the two major factors that are considered for route planning. In section 7.1, the concept of a thematic cost

	32	23		24	25	
31	33	15	34	16	35	26
22	14	8	1	5	9	17
	40	4	0	2	36	
21	13	7	3	6	10	18
30	39	12	38	11	37	27
	29	20		19	28	

Possible movement from Source 0 to pixel number

- Rook's Pattern:** 1,2,3,4
- Bishop's Pattern:** 5,6,7,8
- Knight's Pattern:** 9,10,11,12,13,14,15,16
- Knight31's Pattern:** 17,18,19,20,21,22,23,24
- Knight32's Pattern:** 25,26,27,28,29,30,31,32

Figure 6. Various possible neighbourhood patterns in a 7×7 pixel window. Pixels 1–32 are treated as connected neighbours. Pixel numbers 33–40 are not treated as connected neighbours but are marked only in the context of average thematic cost calculation as mentioned in equations (13) and (14).

map has been introduced, which considers various factors (viz. landslide distribution, landslide hazard zonation, landuse/landcover, drainage order and lithology) in an integrated manner to provide an estimate of the cost per pixel for road development and maintenance. The thematic cost map is a raster map (see figure 5), where the value at each pixel gives the estimated relative cost of moving through that pixel. The thematic cost layer does not include costs due to distance and gradient. It is therefore necessary at this stage to consider and incorporate distance and slope factors.

The NM-cost is the cost of moving from the source to the connected neighbour and is based on the costs of neighbour-distance, gradient and the thematic cost. If the topography is flat (i.e. 0° slope), the topographic surface is isotropic, the gradient cost will be nil, and the NM-cost to move from a source to its connected neighbour is given by:

$$\text{NM-cost} = \text{Neighbour-Distance} \times \text{Thematic Cost} \quad (3)$$

However, if the topography is uneven, particularly in a terrain like the Himalayas, the slope of the terrain varies in different directions. Therefore, the NM-cost must consider this direction dependency (anisotropy), for which, the NM-cost may be given as,

$$\text{NM-cost} = \text{Neighbour-Distance} \times (p \times \text{Thematic Cost} + q \times \text{Gradient Cost}) \quad (4)$$

where, p and q are weights.

Neighbour-distance is the actual distance between successive neighbours in a three-dimensional space. Here, simple Euclidean distance has been used. In the case of raster data, the centre points of various pixels are used for distance computations. Figure 7 schematically describes the method of calculation of distance for any pair of connected pixels in the neighbourhood. In this study, the DEM with a 6 m pixel size has been used for distance computation.

Assuming a square pixel size for the neighbourhood window (figure 7), the distance can be calculated for different neighbourhood connections (Yu *et al.* 2003). For direct horizontal/vertical connection, i.e. the Rook's pattern, the neighbour-distance is:

$$\text{ND}_{(O,P_i)} = \sqrt{\beta^2 + (H_{P_i} - H_O)^2} \text{ where } i = 1 \text{ to } 4 \quad (5)$$

Similarly, for the diagonal direct connection, i.e. the Bishop's pattern, the neighbour-distance is:

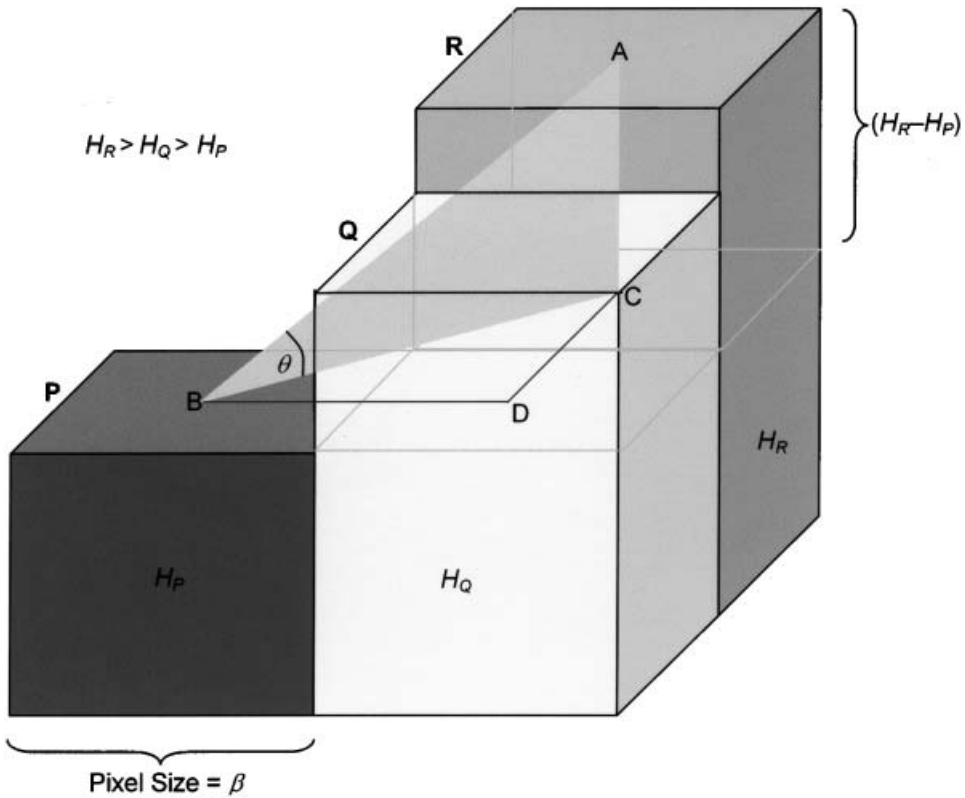
$$\text{ND}_{(O,P_i)} = \sqrt{2\beta^2 + (H_{P_i} - H_O)^2} \text{ where } i = 5 \text{ to } 8 \quad (6)$$

For the Knight's pattern, which is a kind of indirect connection, the neighbour-distance is:

$$\text{ND}_{(O,P_i)} = \sqrt{5\beta^2 + (H_{P_i} - H_O)^2} \text{ where } i = 9 \text{ to } 16 \quad (7)$$

Based on above logic, the neighbour-distances for Knight31's and Knight32's patterns, designed in this study, have been formulated as

$$\text{Knight31's pattern : } \text{ND}_{(O,P_i)} = \sqrt{10\beta^2 + (H_{P_i} - H_O)^2} \text{ where } i = 17 \text{ to } 24 \quad (8)$$



Distance between pixel P and pixel R = AB
 $= (BC^2 + AC^2)^{1/2}$
 $= ((BD^2 + CD^2) + AC^2)^{1/2}$
 $= ((\beta^2 + \beta^2) + AC^2)^{1/2}$
 $= (2\beta^2 + (H_R - H_P)^2)^{1/2}$

Gradient θ = $\tan^{-1}(AC / BC)$
 $= \tan^{-1}((H_R - H_P) / \mu\sqrt{2})$

Figure 7. Concept for calculating distance and gradient between two pixel centres in 3-D. H_R , H_Q , and H_P denote the elevation of pixels P , Q and R , respectively. β is the pixel size. Points A , B , C , and D denote the pixel centres.

$$\text{Knight32's pattern : } ND_{(O,P_i)} = \sqrt{13\beta^2 + (H_{P_i} - H_O)^2} \text{ where } i=25 \text{ to } 32 \quad (9)$$

where ND is the neighbourhood distance between O (source) and pixel P_i (connected neighbour); β is the pixel size, and H_O and H_{P_i} are the elevation of the source and connected neighbour pixels. Pixel numbers corresponding to i are shown in figure 6.

The gradient cost can be defined as the rate of rise or fall along the length of the road with respect to the horizontal (Khanna and Justo 1987). It is usually expressed

as a ratio, e.g. '1 in X ' or '1 vertical unit to X horizontal units'. For hill roads, it has been categorized into three groups by Indian Roads Congress (IRC Manual 2001):

1. Ruling gradient: the gradient that in normal circumstances should not exceed in any part of the road.
2. Limiting gradient: steeper than the ruling gradient and may be used in restricted lengths where the ruling gradient is not feasible.
3. Exceptional gradient: a gradient steeper than the limiting gradient, which may be used in short stretches only in extraordinary situations.

Considering various requirements for smooth movement of vehicles in a hilly terrain, the IRC has recommended maximum values of gradients for different terrain conditions as given in table 2.

The scheme of gradient calculation between two connected neighbours is schematically shown in figure 7. Note that this gradient angle is direction-dependent. A vehicle may move to its connected neighbour according to the permissible gradient. To consider this aspect, the gradient angle has been classified into nine classes, and each class has been assigned a relative weight in the scale of 0–9. A higher weight implies a higher cost arising due to a higher gradient. In this study, due to the ruggedness and high-altitude terrain conditions, the upper limit of the exceptional gradient has been fixed at 12° (which is relatively higher than the IRC recommendation). A gradient greater than 12° has been assigned an infinite cost to eliminate it from the route selection process. The slope classes and corresponding weights are listed in table 3.

For calculating the NM-cost in various neighbourhood patterns, as mentioned earlier the value at each pixel in the thematic cost map gives the estimated relative cost per unit distance of moving through that pixel. While considering movement from a source pixel to the connected neighbour, average thematic costs have been adopted, as the cost of any single pixel may be unrepresentative. In a 3×3 pixel

Table 2. IRC (2001) recommendations on gradients for hill road design.

Classification of gradient	Hilly terrain having elevation more than 3000 m above mean sea level	Hilly terrain upto 3000 m height above mean sea level
(1) Ruling gradient	2.86° (1 in 20.0)	3.43° (1 in 16.7)
(2) Limiting gradient	3.43° (1 in 16.7)	4.00° (1 in 14.3)
(3) Exceptional gradient	4.00° (1 in 14.3)	4.57° (1 in 12.5)

Table 3. Nominal cost values assigned to various gradient classes.

Gradient classes ($^\circ$)	Cost
0–1	1
1–2	2
2–3	3
3–4	4
4–5	5
5–7	7
7–9	8
9–12	9
>12	∞

window, the average thematic cost is simply the average of the two connected pixels. To compute the average costs in the case of indirect connections (5×5 and 7×7 pixel window), the centre points of the connected neighbours have been joined by an imaginary straight line, and all pixels falling on this line have been used to compute the representative thematic cost for the neighbourhood connection in question. For example, referring to figure 6, the thematic cost for a connection between 'O' and '25' has been calculated as an average of costs at pixel numbers 'O', '1', '5', '16', '35' and '25'. The NM-cost for various neighbourhood patterns can be formulated for an anisotropic terrain as detailed below (after Yu *et al.* 2003).

7.3.1 Rook's pattern. In a 3×3 pixel window, the vertical and horizontal moves from the centre pixel may be compared with the movement of the Rook in a game of chess. The NM-cost for this kind of neighbourhood connection (following equation (4)) can be formulated as:

$$\text{NM-cost}_{(O,P_i)} = \sqrt{\beta^2 + (H_{P_i} - H_O)^2} \left(p \times \frac{C_O + C_{P_i}}{2} + q \times f \left(\tan^{-1} \left(\frac{H_{P_i} - H_O}{\beta} \right) \right) \right) \quad (10)$$

where, NM-cost is the neighbourhood movement cost to move from O (source) to pixel P_i (connected neighbour), β is the pixel size, H_O and H_{P_i} are the elevation of source and pixel P_i , respectively, C is the thematic cost to pass through the pixel under consideration, $f(x)$ is a gradient cost function, p and q are weights, and i is the neighbourhood pixel number. Here, $i=1-4$, as in figure 6.

7.3.2 Bishop's pattern. The Bishop's pattern consists of the diagonal movement in a 3×3 pixel window. The NM-cost for this kind of neighbourhood can be formulated as:

$$\text{NM-cost}_{(O,P_i)} = \sqrt{2\beta^2 + (H_{P_i} - H_O)^2} \left(p \times \frac{C_O + C_{P_i}}{2} + q \times f \left(\tan^{-1} \left(\frac{H_{P_i} - H_O}{\sqrt{2}\beta} \right) \right) \right) \quad (11)$$

where $i=5-8$ (see figure 6), and the other parameters are the same as in equation (10).

7.3.3 Knight's pattern. The Knight's pattern can be represented in a 5×5 pixel window. The NM-cost for this kind of neighbourhood can be written as:

$$\text{NM-cost}_{(O,P_i)} = \sqrt{5\beta^2 + (H_{P_i} - H_O)^2} \left(p \times \frac{C_O + C_{Pa} + C_{Pb} + C_{P_i}}{4} + q \times f \left(\tan^{-1} \left(\frac{H_{P_i} - H_O}{\sqrt{5}\beta} \right) \right) \right) \quad (12)$$

where $i=8-16$ (see figure 6). The value of a and b varies depending upon the neighbouring pixel under consideration, e.g. for $i=9$, $a=2$ and $b=5$, and so on.

7.3.4 Knight31's pattern. This is the newly designed neighbourhood pattern for a 7×7 pixel window. The NM-cost for this kind of neighbourhood has been

formulated as:

$$\text{NM-cost}_{(O,P_i)} = \sqrt{10\beta^2 + (H_{P_i} - H_O)^2} \left(p \times \frac{C_O + C_{Pa} + C_{Pb} + C_{Pc} + C_{Pd} + C_{P_i}}{6} + q \times f \left(\tan^{-1} \left(\frac{H_{P_i} - H_O}{\sqrt{10\beta}} \right) \right) \right) \quad (13)$$

where $i=17-24$ (see figure 6). The value of a , b , c and d varies as it depends on the neighbouring pixel under consideration, e.g. for $i=17$, $a=2$, $b=5$, $c=9$ and $d=36$, and so on.

7.3.5 Knight32's pattern. This is another newly designed neighbourhood pattern for a 7×7 pixel window. The NM-cost for this kind of neighbourhood has been formulated as:

$$\text{NM-cost}_{(O,P_i)} = \sqrt{13\beta^2 + (H_{P_i} - H_O)^2} \left(p \times \frac{C_O + C_{Pa} + C_{Pb} + C_{Pc} + C_{Pd} + C_{P_i}}{6} + q \times f \left(\tan^{-1} \left(\frac{H_{P_i} - H_O}{\sqrt{13\beta}} \right) \right) \right) \quad (14)$$

where $i=25-32$. The value of a , b , c and d varies and depends on the neighbouring pixel under consideration, e.g. for $i=25$, $a=1$, $b=5$, $c=16$ and $d=35$, and so on (see figure 6).

In this study, p and q are assigned values of 1 and 8, respectively. This is in view of the fact that while calculating the thematic cost layer, a weight of 8 has been given to LHZ (see table 1), and it appears reasonable that a similar weight (=8) be given to gradient cost to have an equivalent weight consideration.

7.4 Selection of least-cost route

In this paper, the classical Dijkstra algorithm, has been used to determine the least-cost path, as the main emphasis here is on the development of a methodology for route planning in landslide-prone terrain. Detailed explanation of this algorithm can be found in a number of publications (e.g. Horowitz *et al.* 2002, Rees 2004, etc.). The least-cost route between a source and a destination points can be determined using Dijkstra's Algorithm, named after its inventor, the Dutch computer scientist Edsger Dijkstra. This algorithm is specifically written for a node-based network. To implement the algorithm in a raster-based analysis, the centre-point of each pixel has been considered as a node in the network.

According to this algorithm, each pixel in a raster framework should contain two basic types of information: NM-cost, which comprises neighbourhood distance, gradient and thematic costs; and a pointer that identifies the connected pixels. This information are updated in an iterative process to determine the least-cost path from a designated source to the destination.

The methodology for route planning adopted in this study has been implemented using a dedicated software written in C++. The outputs from the software have been suitably interfaced with ILWIS GIS. Details of the software can be found in Saha (2004).

8. Testing of route planning methodology

In previous sections, the methodology developed for finding the least-cost route in a landslide-prone terrain has been described. The procedure is computationally

intensive and time-consuming. Therefore, to test the concept and the methodology in finding safe routes in a landslide-prone rugged terrain, a few test areas of size $1.5 \text{ km} \times 1.5 \text{ km}$, with different terrain conditions and landslide susceptibility, have been selected. The test results on some of these sites are presented next.

8.1 Case of a major landslide and adjacent minor landslides

This example considers the case of major and minor landslides occurring in adjacent areas such that the source and destination points are located across the set of landslides. Figure 8 shows the test area, which is situated west of the Gopeshwar town. There is a major landslide along with a debris flow channel that carries the debris to the river valley in the east.

Consider the case that the entire landslide and the associated debris flow track is unsuitable for route location and therefore must be avoided. For such a situation, a buffer zone can be created around the landslide and debris flow track. The entire zone can be assigned a high value in the thematic cost layer. The source and destination points have been selected at nearly the same elevation (approximately 1600 m) on either side of the set of major and minor landslides (figure 8). The computed route when only topography is considered predominantly follows the contour line and crosses right through the middle of the minor and major landslides. When both topography and thematic cost are used, the computed route passes through the minor landslides but avoids the major landslide and its buffer zone, though it takes a longer distance to reach the destination point.

Consider another possibility that only the main landslide area is to be avoided, and the associated debris flow track on the east can be treated as minor landslide across which a suitable structure (e.g. a suspension bridge) can be constructed. In this case, the buffer zone is created only around the main landslide area (figure 9). A set of source and destination points has been selected on the northwest and southeast of the major landslide (figure 9). It is found that when only topography is considered, the route passes through the major landslide. On the other hand, when both the topography and the thematic cost are considered, the computed route avoids the major landslide and passes over the debris flow track (over which the feasibility of a suitable structure has been taken into consideration).

8.2 Case of significant regional variation in thematic costs

In this example, the area selected is the same as in case 1, but the area possesses a large regional variation in thematic cost values, as indicated by yellow–orange–red pixels in the southeastern part and blue–green pixels generally in the northwestern part. The task considered here is to join the southwest corner with the northeast corner. Figure 10 shows the thematic cost map draped over the shaded relief model to represent the terrain. The existing landslide zones are assigned higher costs; these are mainly represented in red. A 50 m buffer zone around major landslides is also provided to keep a safe distance for passing a route. Contour lines are shown in pseudo-colours to highlight the topography.

As in the previous case, the least-cost path found by taking into account only topography is marked in blue. For the same source and destination points, another least-cost path has been computed by considering the topography as well as the thematic cost, and is marked in yellow. It can be seen that the path shown in blue

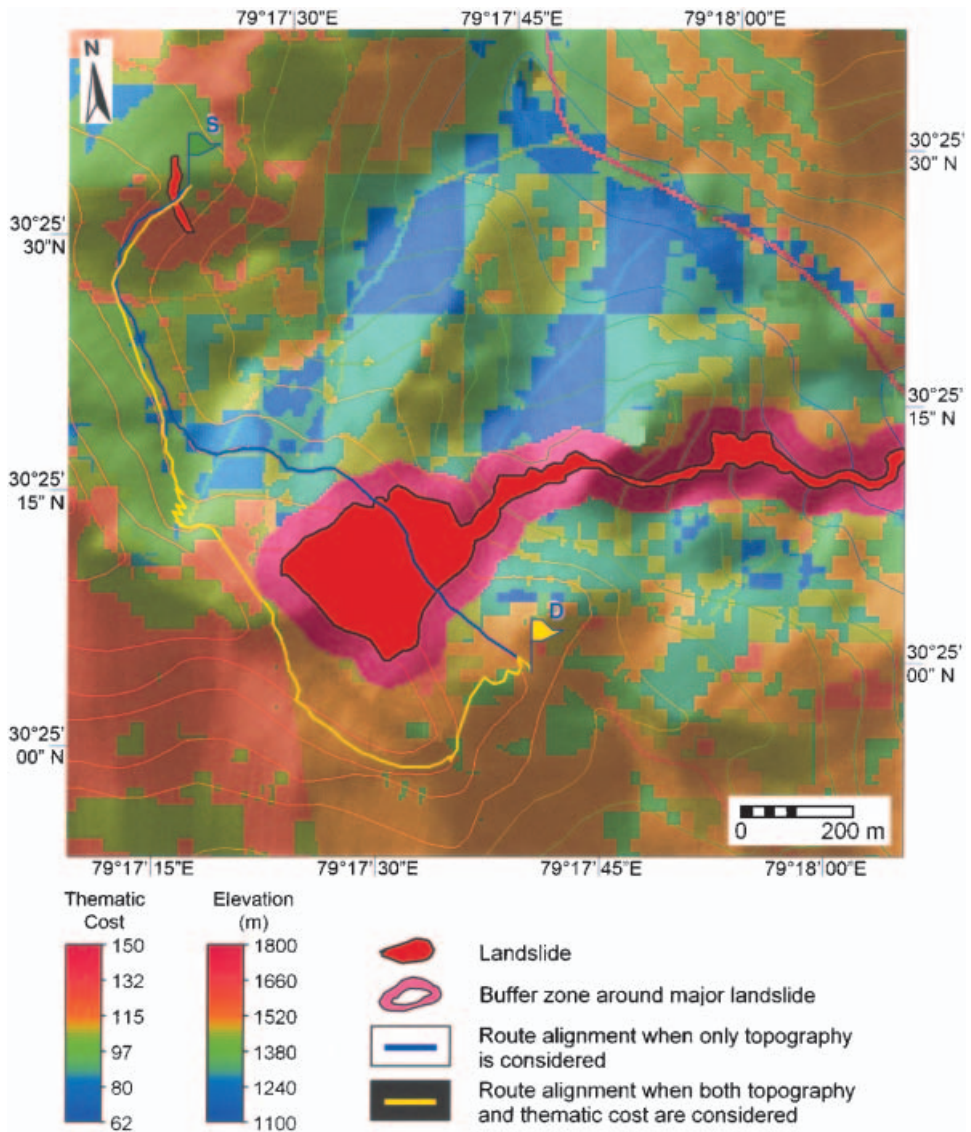


Figure 8. Comparison of alternate route alignments in case of a major landslide and adjacent minor landslide. Note that when only topography is considered, the route passes through the landslides, whereas when both the topography and thematic costs are considered, the route avoids the major landslide and buffer zone around it (S: source; D: destination).

mostly passes through areas with higher values of thematic cost, even crossing the major landslide twice on its way to destination. In contrast, the path shown in yellow avoids the higher thematic cost areas and mostly passes through the blue and green regions, i.e. the lower thematic cost value regions.

9. Concluding remarks

Based on the working examples, it can be stated that the proposed GIS-based route planning methodology appears to have several merits, which can be enumerated as follows:

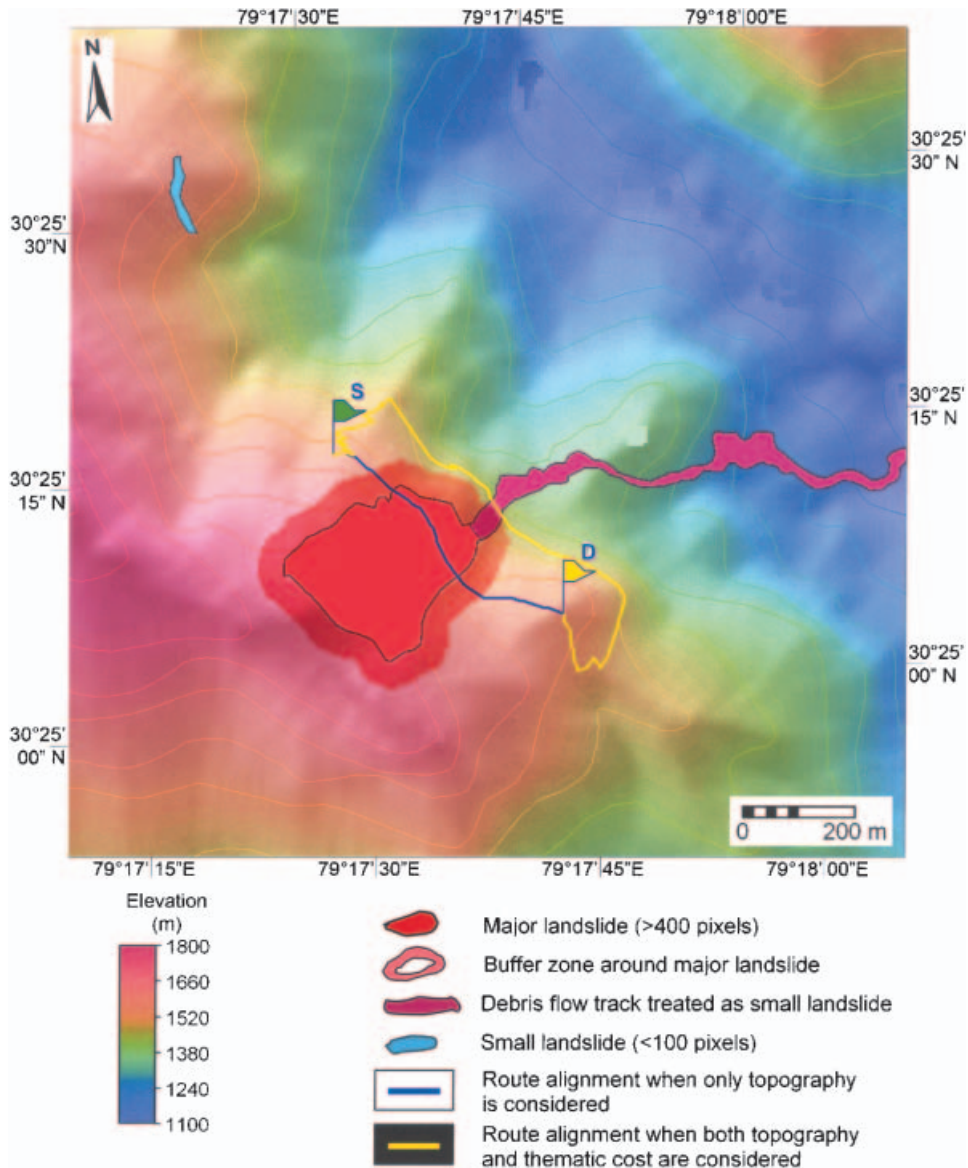


Figure 9. Another possibility described in the previous case (see Figure 8). In this case, the debris flow track is treated as a minor landslide, where construction of a bridge can allow debris to pass through. Note that when only topography is considered, the route passes through the major landslide, whereas when both the topography and thematic costs are considered, the route avoids the major landslide and buffer zone around it, and passes through the debris flow channel (S: source; D: destination).

1. The approach developed here has been successfully tested for landslide-prone terrain. It has been observed that the routes identified by the proposed methodology in the high-altitude, rugged Himalayan terrain with markedly different landslide susceptibility conditions pass through relatively safe areas avoiding major landslides. Thus, the planning of a road in hilly area using this methodology will result in a safer and cost-effective route involving lower recurring costs for road development and maintenance.

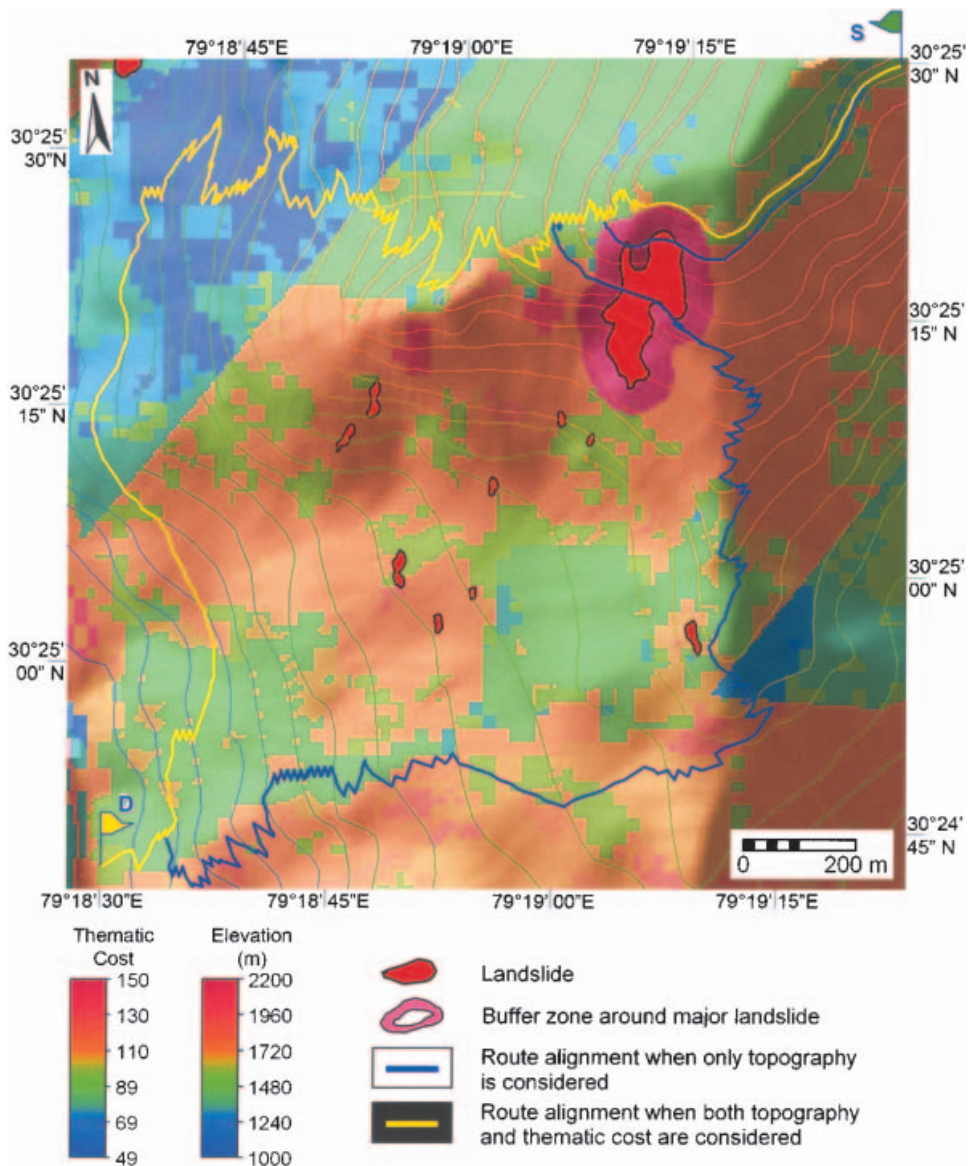


Figure 10. Example showing alternative route alignments, given the task that the northeast corner has to be joined with the southwest corner. When only topography is considered, the alignment passes through higher thematic cost zones and landslide zones; when both the topography and thematic cost are considered, the route passes through mainly lower thematic cost zones and avoids the landslide areas.

2. The computer-assisted methodology of route planning is very fast in comparison with the conventional manual practice. The working examples show that for a test area of $1.5 \text{ km} \times 1.5 \text{ km}$, the computer-based, least-cost, route-finding process takes about 13 min, and in contrast, the same process may take many days by the manual approach, even if all data are to hand. The efficiency of the proposed algorithm can further be increased as the processing technology advances.

3. In the GIS-based methodology, it is possible to integrate and analyse various parameters related to road development and maintenance at the same time. For this purpose, the concept of thematic cost has been introduced in this study. In the manual method, it is difficult to consider a large number of parameters at the same time to conduct a purposeful analysis.
4. In manual route-alignment practice, it is quite possible that an alternate best route becomes unknowingly overlooked. In contrast, this methodology uses Dijkstra's Algorithm to find the least-cost path. The algorithm is intelligent, fast and efficient, and considers all possible combinations of routes between the source and the destination points. Therefore, the least-cost path found by the algorithm would provide the best option with certainty.
5. The GIS-based methodology considers a gradient for various direction-dependent connected neighbours, thematic cost and distance in a three-dimensional space. The path gradient can be adjusted as per the requirements, depending upon the terrain conditions. Hence, it should be possible to design a more realistic route in an automated way by merely changing some of the parameters, as appropriate.

Finally, it may be emphasized that the thrust of this research is on the methodology development. The list of factors and their weighting rating can be modified and adjusted, depending upon the local conditions in an area. A further increase in the window size to 9×9 pixels or a higher matrix would yield smoother paths with a gradual and realistic variation in the path gradient, although this would increase the computational complexity.

Acknowledgements

AKS is grateful to the Council of Scientific and Industrial Research (CSIR), India and the German Academic Exchange Service (DAAD), Germany for providing fellowships to carry out this research work.

References

- AKINYEDE, J.O., 1990, A geotechnical GIS concept for highway route planning. *ITC Journal*, **3**, pp. 262–269.
- ARONOFF, S., 1989, *Geographic Information Systems: A Management Perspective* (Ottawa: WDL).
- ARORA, M.K., DAS GUPTA, A.S. and GUPTA, R.P., 2004, An artificial neural network approach for landslide hazard zonation in the Bhagirathi (Ganga) Valley. Himalayas. *International Journal of Remote Sensing*, **25**(3), pp. 559–572.
- ARORA, M.K. and MATHUR, S., 2001, Multi-source classification using artificial neural network in a rugged terrain. *GeoCarto International*, **16**(3), pp. 37–44.
- CHAVEZ, P.S. Jr., 1988, An improved dark object subtraction technique for atmospheric correction of multispectral data. *Remote Sensing of Environment*, **24**, pp. 459–479.
- COLLISCHONN, W. and PILAR, J.V., 2000, A direction dependent least-cost-path algorithm for roads and canals. *International Journal of Geographical Information Science*, **14**(4), pp. 397–406.
- DIJKSTRA, E.W., 1959, A note on two problems in connection with graphs. *Numerische Mathematik*, **1**, pp. 269–271.
- DOUGLAS, D.H., 1994, Least-cost path in GIS using an accumulated-cost surface and slope lines. *Cartographica*, **31**, pp. 37–51.

- ELLIS, M.C., 1990, Analytical free-range route planning 'G-Route' GIS simulation model. *Technical Note Internal Publication ITC*, Enschede, The Netherlands.
- FELDMAN, S.C., PELLETIER, R.E., WALSER, E., SMOOT, J.C. and AHL, D., 1995, A prototype for pipeline routing using remotely sensed data and geographic information system analysis. *Remote Sensing of Environment*, **53**, pp. 123–131.
- FRITZ, S. and CARVER, S., 1998, Accessibility as an important wilderness indicator: Modelling Naismith's Rule. Available online at: <http://www.geog.leeds.ac.uk/papers/98-7/>.
- GUPTA, R.P., 2003, *Remote Sensing Geology*, 2nd edition (Berlin: Springer).
- GUPTA, R.P. and JOSHI, B.C., 1990, Landslide hazard zonation using the GIS approach—a case study from the Ramganga Catchment, Himalayas. *Engineering Geology*, **28**, pp. 119–131.
- HOROWITZ, E., SAHNI, S. and RAJASEKARAN, S., 2002, *Fundamentals of Computer Algorithms* (New Delhi: Galgotia).
- IRC Manual, 2001, Recommendations about the Alignment Survey and Geometric Design of Hill Roads, 2nd revision. *The Indian Roads Congress*, IRC: 52–2001.
- KHANNA, S.K. and JUSTO, C.E.G., 1987, *Highway Engineering*, 6th edition (Roorkee: Nem Chand & Bros).
- LEE, J. and STUCKY, D., 1998, On applying viewshed analysis for determining least-cost paths on digital elevation models. *International Journal of Geographical Information Science*, **12**(8), pp. 891–905.
- MUSA, M.K.A. and MOHAMED, A.N., 2002, Alignment and locating forest road network by best-path modeling method. Available online at: <http://www.gisdevelopment.net/aars/acrs/2002/for/092.pdf>.
- NAGARAJAN, R., MUKHERJEE, A., ROY, A. and KHIRE, M.V., 1998, Temporal remote sensing data and GIS application in landslide hazard zonation of part of Western Ghat, India. *International Journal of Remote Sensing*, **19**(4), pp. 573–585.
- REES, W.G., 2004, Least-cost paths in mountainous terrain. *Computers & Geosciences*, **30**, pp. 203–209.
- SAHA, A.K., 2004, GIS-based study for route planning in landslide susceptible terrain. PhD thesis, IIT Roorkee, India.
- SAHA, A.K., ARORA, M.K., CSAPLOVICS, E. and GUPTA, R.P., 2005 a, Land cover classification using IRS LISS III imagery and DEM in a rugged terrain: A case study in Himalaya. *GeoCarto International*, **20**(2), pp. 33–40.
- SAHA, A.K., GUPTA, R.P. and ARORA, M.K., 2002, GIS-based landslide hazard zonation in the Bhagirathi (Ganga) Valley, Himalayas. *International Journal of Remote Sensing*, **23**(2), pp. 357–369.
- SAHA, A.K., GUPTA, R.P., SARKAR, I., ARORA, M.K. and CSAPLOVICS, E., 2005 b, An approach for GIS-based statistical landslide susceptibility zonation—with a case study in the Himalayas. *Landslides*, **2**, pp. 61–69.
- SCHNEIDER, K. and ROBBINS, P. (Eds.), 1998, *Modeling Access to Health Care: Anisotropic Cost Distance, GIS and Mountain Environments, Explorations in Geographic Information Systems Technology*, Vol. 5 (Geneva: UNITAR).
- SOLKA, J.L., PERRY, J.C., POELLINGER, B.R. and ROGERS, G.W., 1995, Fast computation of optimal paths using a parallel Dijkstra Algorithm with embedded constraints. *Neurocomputing*, **8**, pp. 195–212.
- STRAHLER, A.N., 1964, Quantitative geomorphology of drainage basins and channel networks. Section 4, pp. 41–75. In V.T. Chow, (Ed). *Handbook of Applied Hydrology* (New York: McGraw-Hill).
- TANIMETO, S.L., 1987, *The Elements of Artificial Intelligence—An Introduction Using LISP* (New York: Computer Science Press).
- VALDIYA, K.S., 1980, *Geology of Kumaun Lesser Himalaya* (Dehradun: Wadia Institute of Himalayan Geology).

- VARNES, D.J., 1984, *Landslide Hazard Zonation: A Review of Principles and Practice* (Paris: UNESCO).
- VOOGD, H., 1983, *Multi-Criteria Evaluations for Urban and Regional Planning* (London: Princeton University).
- XU, J. and LATHROP, R.G., 1994, Improving cost-path tracing in a raster data format. *Computers & Geosciences*, **20**(10), pp. 1455–1465.
- YU, C., LEE, J. and MUNRO-STASIUK, M.J., 2003, Extensions to least-cost path algorithms for roadway planning. *International Journal of Geographical Information Science*, **17**(4), pp. 361–376.

Copyright of International Journal of Geographical Information Science is the property of Taylor & Francis Ltd and its content may not be copied or emailed to multiple sites or posted to a listserv without the copyright holder's express written permission. However, users may print, download, or email articles for individual use.